

Dynamics of seismogenic volcanic extrusion at Mount St Helens in 2004–05

Richard M. Iverson¹, Daniel Dzurisin¹, Cynthia A. Gardner¹, Terrence M. Gerlach¹, Richard G. LaHusen¹, Michael Lisowski¹, Jon J. Major¹, Stephen D. Malone², James A. Messerich³, Seth C. Moran¹, John S. Pallister¹, Anthony I. Qamar^{2,‡}, Steven P. Schilling¹ & James W. Vallance¹

The 2004–05 eruption of Mount St Helens exhibited sustained, near-equilibrium behaviour characterized by relatively steady extrusion of a solid dacite plug and nearly periodic shallow earthquakes. Here we present a diverse data set to support our hypothesis that these earthquakes resulted from stick-slip motion along the margins of the plug as it was forced incrementally upwards by ascending, solidifying, gas-poor magma. We formalize this hypothesis with a dynamical model that reveals a strong analogy between behaviour of the magma–plug system and that of a variably damped oscillator. Modelled stick-slip oscillations have properties that help constrain the balance of forces governing the earthquakes and eruption, and they imply that magma pressure never deviated much from the steady equilibrium pressure. We infer that the volcano was probably poised in a near-eruptive equilibrium state long before the onset of the 2004–05 eruption.

Silicic volcanoes are famous for capricious behaviour¹, but the dome-building eruption of Mount St Helens (MSH) that began in October 2004 and continues today has exhibited prolonged, near-equilibrium behaviour that affords unique opportunities for understanding volcano dynamics. A remarkable feature of the eruption has been the persistence of nearly steady, solid-state extrusion ($1\text{--}2\text{ m}^3\text{ s}^{-1}$) accompanied by nearly periodic earthquakes with shallow ($<1\text{ km}$) focal depths. The repetitive nature of these earthquakes implies the existence of a non-destructive seismic source, and it provides an exceptional opportunity to link seismicity and extrusion dynamics^{2,3}. Here we summarize seismic, geodetic, photogrammetric, petrologic, geochemical and thermal data collected during the 2004–05 MSH eruption, and we hypothesize a mechanistic link between solid-state extrusion and nearly periodic earthquakes. A new mathematical model formalizes our hypothesis, and reveals a strong analogy between the behaviour of MSH and that of a variably damped oscillator. We exploit this analogy to probe unobserved aspects of eruption dynamics.

Eruptive behaviour and seismicity

Although MSH erupted explosively on 18 May 1980, dome-building activity that began in 2004 is consistent with the volcano's recent geologic history⁴. Over the past $\sim 4,000$ yr, MSH has extruded rock at a mean rate of $\sim 0.2\text{ m}^3\text{ s}^{-1}$ while constructing a 26 km^3 edifice composed primarily of andesite and dacite lava flows and domes and their detritus (Supplementary Fig. 1). From 1980 to 1986, a dacite dome grew episodically in the 1980 crater, and its volume ultimately reached $74 \times 10^6\text{ m}^3$ (ref. 5). From 1987 to 2004, MSH did not erupt, although at least six phreatic explosions occurred from 1989 to 1991⁶. Recurrent seismicity at depths of 2–8 km in the late 1980s and 1990s may have been associated with magma recharge, but did not lead to eruptions⁷.

The current eruption began on 1 October 2004, when a small explosion formed a $\sim 20\text{-m}$ -diameter vent through a $\sim 150\text{-m}$ -thick glacier that had grown in the southern part of the MSH crater since

1986^{8–10}. The explosion was preceded by 8 days of increasingly intense seismicity at depths $<1\text{ km}$, but deeper seismicity did not occur then and has not occurred subsequently. By 11 October, explosions had largely ceased, seismic energy release had decreased to a rate about one-tenth that of the preceding two weeks, and extrusion of solid dacite had begun⁸.

The newly extruded dacite formed a series of spines with freshly exposed surfaces coated with fault gouge (that is, granulated rock bearing multiple generations of subparallel striations and slickensides). The most prominent spine emerged in winter 2005 and had a remarkably smooth, symmetrical whaleback form (Fig. 1 and Supplementary Movies 1 and 2), but most spines were partly obscured as they pushed past glacial ice and previously extruded rock.

Although spines repeatedly formed and disintegrated, extrusion rates remained roughly constant. The volumetric extrusion rate inferred from intermittent photogrammetric surveys was initially $\sim 6\text{ m}^3\text{ s}^{-1}$, but by December 2004 it had declined to a value of $1\text{--}2\text{ m}^3\text{ s}^{-1}$ that was sustained for the ensuing year (Fig. 2). (Supplementary Information describes measurement methods.) Similarly, the speed of plug emergence from the vent was nearly constant over timescales ranging from several minutes to several months, and was typically $3\text{--}6\text{ m d}^{-1}$. By 15 December 2005 the volume of the resulting new lava dome was $\sim 73 \times 10^6\text{ m}^3$, implying that the average MSH extrusion rate from 1980 to 2005 was similar to the $0.2\text{ m}^3\text{ s}^{-1}$ average for the past 4,000 yr.

Small earthquakes (coda duration magnitude, $M_D < 2$) that accompanied solid-state extrusion occurred so regularly that we dubbed them 'drumbeats' (Fig. 3). The period between successive drumbeats shifted slowly with time, but was nearly always 30–300 s (Fig. 2). Seismograms showed that drumbeat waveforms typically had impulsive, high-frequency onsets and low-frequency codas, similar to those of other 'hybrid' volcanic earthquakes^{2,3}. Accurate location of drumbeat hypocentres was hindered by the geologic and topographic complexity of the MSH crater and the small number

¹US Geological Survey, Cascades Volcano Observatory, 1300 SE Cardinal Ct. #100, Vancouver, Washington 98683, USA. ²Earth and Space Sciences, University of Washington, Seattle, Washington 98195, USA. ³US Geological Survey, Denver Federal Center, Box 25046, Lakewood, Colorado 80225, USA.

[‡]Deceased.

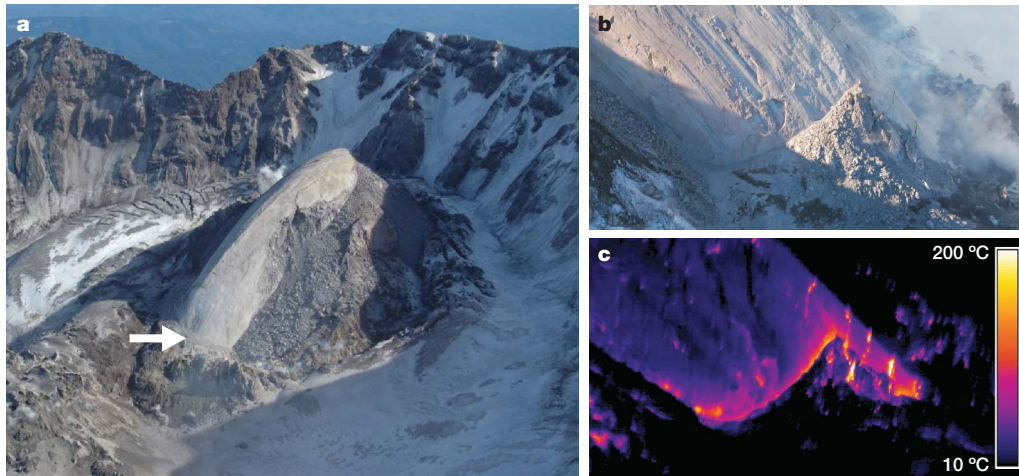


Figure 1 | Images of the whaleback spine and the surrounding MSH crater in February 2005. **a**, Oblique aerial view from the northwest. The arrow indicates the vent from which the whaleback emerged. The horizontal length

of smooth whaleback is about 380 m. **b**, Close-up view of the gouge-covered surface of the spine where it emerged from the vent, viewed from the northeast. **c**, Thermal infrared view from a perspective similar to **b**.

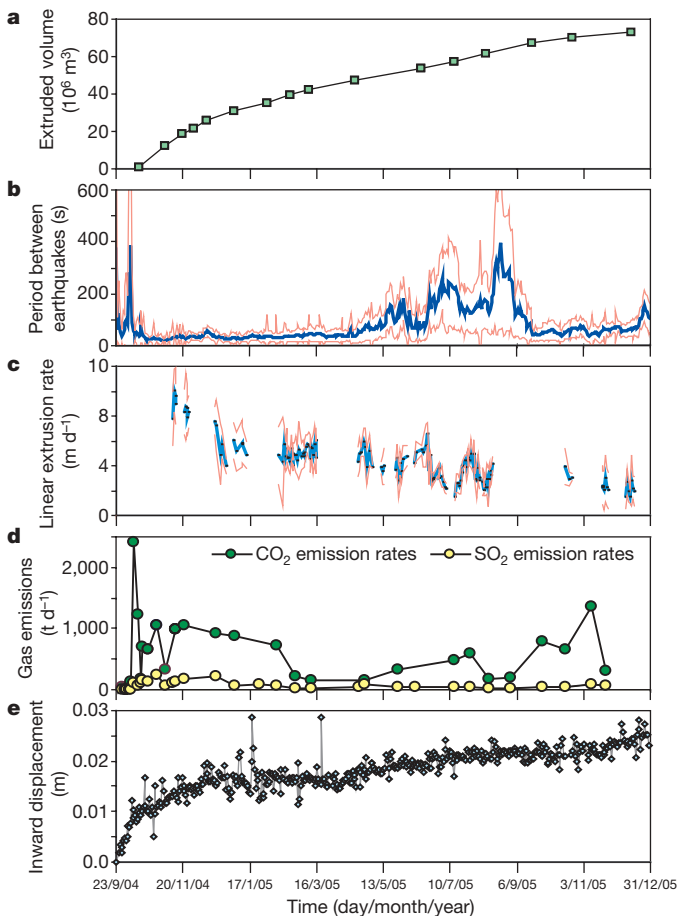


Figure 2 | Time-series data summarizing eruption behaviour. **a**, Cumulative volume of extruded rock. **b**, Mean period (± 1 s.d.) between successive earthquakes recorded at station YEL (Supplementary Fig. 1), computed for 24-h sampling windows. **c**, Linear extrusion rate ± 1 s.d., inferred from repeat photography. Data gaps appear where clouds obscured the view or equipment malfunctioned. **d**, Emission rates of gaseous CO_2 and SO_2 . **e**, Cumulative inward displacement of continuous GPS station JRO1, located 9 km north of the vent (Supplementary Fig. 1). Regional displacements due to plate tectonic motion (constrained by regional GPS) have been removed from data.

of crater seismometers (Supplementary Fig. 1), but within resolution limits (~ 100 m), all drumbeats originated at depths < 1 km directly around or beneath the growing dome. Irregularly interspersed with the drumbeats were smaller and larger earthquakes ($M_D \leq 3.4$) with differing seismic signatures, but these earthquakes rarely had any effect on drumbeat occurrence.

Extruded rock, gouge and magma

Sampling of fault gouge coating the spines and of the dacite beneath the gouge was accomplished mostly by dredging from a helicopter. The gouge thickness was typically ~ 1 m and grain sizes were generally 0.001–10 mm. The gouge composition was similar to that of the newly erupted dacite, but included some constituents like those of pre-1980 MSH rocks. Airborne measurements of infrared radiation emitted by gouge emerging from the vent typically yielded temperatures of ~ 200 °C (Fig. 1), and temperatures within fissures penetrating through the gouge were no higher than 730 °C. Initial results of rheological experiments showed that even at a temperature of 1,000 °C, the new dacite deformed mostly by brittle failure rather than viscous flow, accentuating the potential for strain localization,

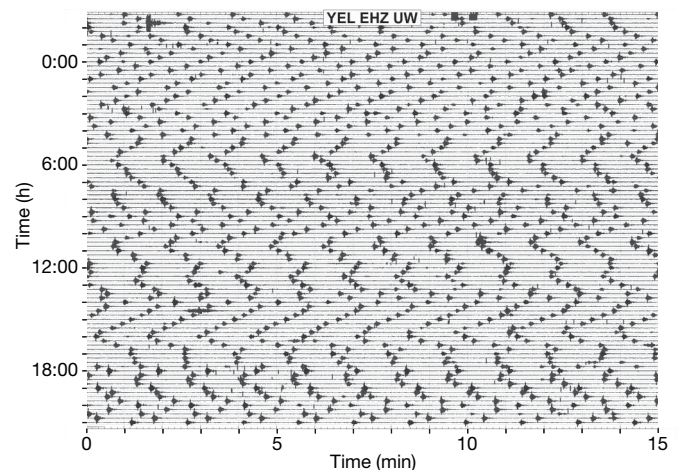


Figure 3 | Sample 24-h seismogram, illustrating regular occurrence of drumbeat earthquakes. Graph shows seismicity recorded at station YEL, located 1.5 km north of the 2004–05 vent (Supplementary Fig. 1). Time begins at 21:00 UTC on 1 December 2005, and scrolls from left to right and then top to bottom. Earthquake magnitudes were roughly 0.5–1 during this interval. (YEL/EHZ/UW is the station/component/network code for this seismic station.)

wear, and fault-gouge development^{11,12}. Room-temperature ring-shear tests on gouge specimens 7 cm thick under normal stresses of 86–191 kPa yielded steady-state (large-strain) friction coefficients μ ranging from 0.42 to 0.47, peak (small-strain) friction coefficients 1–9% larger than μ , and a roughly logarithmic decline of μ as displacement rates increased from about 10^{-6} to 10^{-4} m s⁻¹ (ref. 13).

The mineralogy and major- and trace-element compositions of the newly extruded dacite are similar to those of the youngest rocks composing the 1980s dome at MSH¹¹. Moreover, Fe-Ti oxide equilibration temperatures of samples collected in November 2004 are like those of the 1986 MSH dacites (840–850 °C). Owing to these similarities and low magmatic gas emissions, we infer that much of the 2004–05 dacite originated from magma remaining in the reservoir tapped by the 1980s eruption. Nonetheless, the long-term magma history may be complex, as extruded rocks contain phenocrysts that range widely in age and inferred source depth¹¹.

Petrologic data imply that magma solidification occurred at depths <1 km. The groundmass of the newly erupted dacite consists largely of a microlite mosaic of quartz or tridymite, sodic plagioclase and anorthoclase, with minor amounts (<15%) of high-silica rhyolite glass. The glass composition plots between the 0.1 and 50 MPa cotectics of the modified quartz–albite–orthoclase phase diagram for MSH dacites¹⁴, and the presence of tridymite further constrains the late stages of solidification to pressures of 10–20 MPa (equivalent to lithostatic pressures at depths of ~0.5–1 km)¹¹.

Volcanic gases intermittently measured by aircraft¹⁵ included CO₂, SO₂ and H₂S, and these measurements indicated the presence of magma with exsolved gas content lower than that at MSH in the early 1980s. Following the explosion of 1 October 2004, gas emission rates were <150 t d⁻¹ CO₂ and <8 t d⁻¹ H₂S, and after extrusion began on 11 October, mean emission rates increased to about 650 t d⁻¹ CO₂ and 100 t d⁻¹ SO₂ (Fig. 2). The cumulative CO₂ released through July 2005 (about 190 kt) indicates that the 2004–05 magma was gas-saturated at 8 km depth, and it constrains the gas volume fraction at that depth to <2% (assuming that the 2004–05 and 1980–86 MSH dacites have similar water contents of ~5 wt% in the rhyolitic melt fractions^{14,16,17}). Calculations using established methods¹⁶ indicate that the gas volume fraction grew during magma ascent, reached about 50% at ~1 km depth, where solidification began, and averaged ~12% between 1 and 8 km. Allowing for inevitable gas separation during extrusion, these results are consistent with observed vesicle volume fractions of 11–34% in samples of the 2004–05 dacite¹¹.

Geodetic constraints on magma source

Measured displacements of the volcano flanks and adjacent areas imply that the volume of magma evacuated from depths <10 km was considerably less than the volume of extruded rock. No evidence of systematic pre-eruption surface displacement was detected by GPS (Global Positioning System) surveys in 2000 and 2003 of a 40-station network centred on the volcano, nor by continuous operation of GPS station JRO1, located 8 km north of the volcano (Supplementary Fig. 1). Seismicity that heralded the eruption onset was accompanied by only centimetre-scale downward and inward surface displacements at JRO1 (Fig. 2). The measured displacement pattern corresponds well with predictions of an elastic half-space model¹⁸ that assumes pressure decrease within a vertically oriented, prolate spheroidal cavity with a mean depth of 8 km and volume loss of ~2 × 10⁷ m³ from 1 October 2004 to 25 November 2005. This apparent volume loss is less than one-third of the volume of rock extruded during the same period, and most of the apparent volume loss occurred before the onset of nearly steady extrusion in December 2004 (Fig. 2), implying that magma recharge from a deep (>10 km) source accompanied extrusion.

Mechanical hypothesis

To examine connections between solid-state extrusion and persistent drumbeat earthquakes at MSH, we consider mechanical processes

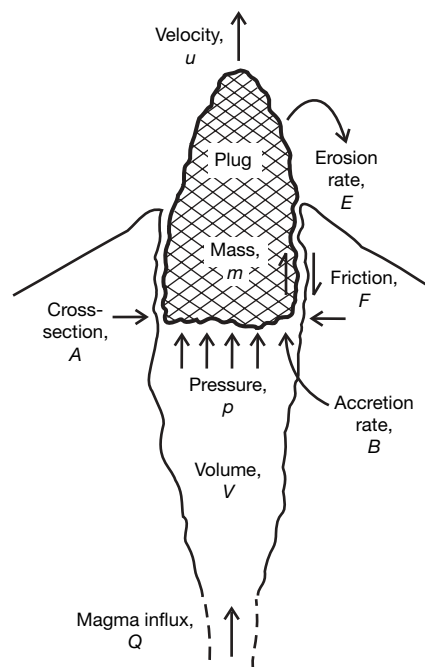


Figure 4 | Diagram of model. See text for details.

that differ from those addressed by models of erupting fluid magma^{19,20} or seismogenic motion of volcanic fluids²¹. We hypothesize that repetitive stick-slip motion along the margins of the extruding solid plug is responsible for generating drumbeat earthquakes, and that the stick-slip cycles themselves represent mechanical oscillations about equilibrium. Although prior studies have invoked stick-slip behaviour to explain cyclical behaviour during volcanic eruptions^{12,22–24}, they have not quantified the causes and character of stick-slip dynamics.

Quantification of our hypothesis requires identification of pertinent assumptions, parameters and variables (Fig. 4). We assume that magma flows into the base of an eruptive conduit (at 8 km depth, inferred from 1980–2000 seismicity) at a steady rate $Q = 2 \text{ m}^3 \text{ s}^{-1}$. An effectively rigid plug of solidified magma occupies the conduit's upper ~0.5 km (inferred from petrologic and seismic data), but the position of the plug base may change owing to upward motion and basal accretion at mass rate ρB , where ρ is magma bulk density and B is the volumetric rate of magma solidification. We assume that the plug bulk density ρ_r is constant ($2,000 \text{ kg m}^{-3}$, inferred from dome-rock specimens) and that the plug mass m can evolve owing to differences between ρB and $\rho_r E$, where E is the volumetric rate of surface erosion. For simplicity we assume that $\kappa = \rho B - \rho_r E$ is constant; thus $m = m_0 + \kappa t$, where m_0 is the initial plug mass and t is time. We estimate the horizontal cross-sectional area of the plug base, A , to be $30,000 \text{ m}^2$ (obtained by dividing $Q = 2 \text{ m}^3 \text{ s}^{-1}$ by the linear extrusion velocity $7 \times 10^{-5} \text{ m s}^{-1}$); this A implies an effective vent diameter of ~200 m, consistent with results of photogrammetric analyses (Supplementary Movie 1). We estimate the magma compressibility α_1 as 10^{-7} Pa^{-1} (appropriate for a 12% mean bubble content²⁵), and estimate the conduit wall compliance α_2 as 10^{-9} Pa^{-1} (appropriate for fractured rock). Values of α_1 and α_2 are not tightly constrained, but $\alpha_1 > \alpha_2$ is virtually certain, and we therefore infer that magma compression dominates elastic strain as the system pressurizes. Extrusion is resisted by the friction force F and the plug weight mg , where g is the acceleration due to gravity. Dependent variables that evolve during extrusion are the upward plug velocity u , magma pressure against the base of the plug p , mean magma density ρ , and volume of the magma-filled conduit V .

If drumbeat earthquakes result from incremental slip along the margins of the plug, then the slip distance per drumbeat is $\bar{u}T$, where

\bar{u} is the mean extrusion velocity and T is the drumbeat period. On this basis, we infer that individual slip events typically involve plug displacements of ~ 5 mm at earthquake focal depths. Calculations test whether our mechanical hypothesis is consistent with periodic displacements of this size, although such small, brief displacements were not measurable by our instruments.

Mathematical model

We formalize our hypothesis with a model based on the following: one-dimensional conservation laws describing the evolving mass and vertical momentum of the solid plug and underlying magma; constitutive equations defining F , α_1 and α_2 ; and the assumption that Q is constant. For these conditions the governing equations reduce to:

$$\frac{du}{dt} = -g + \frac{1}{m_0 + \kappa t} (pA - \kappa u - F) \quad (1)$$

$$\frac{dp}{dt} = \frac{-1/V}{\alpha_1 + \alpha_2} (Au + RB - Q) \quad (2)$$

$$\frac{dV}{dt} = \frac{\alpha_1}{\alpha_1 + \alpha_2} (Au + RB - Q) + Q - B \quad (3)$$

where $R = 1 - (\rho/\rho_r)$ is a nearly constant coefficient determined by an isothermal equation of state, and all other variables and parameters are defined above. (Detailed derivations and discussions of these equations are provided in Supplementary Information.)

If the plug mass is constant and the basal solidification rate equals the magma influx rate, equations (1)–(3) have an equilibrium solution describing steady plug extrusion with constant magma pressure and density, conduit volume, and plug friction ($u = (Q - RB)/A$, $p = (m_0 g + F)/A$, $\rho = \rho_0$, $V = V_0$). Key dynamics questions are whether such steady states are stable, whether persistently oscillating states that can produce drumbeat earthquakes are probable, and whether initial disequilibrium states are attracted to steady or unsteady states.

Insight is gained by approximating R as constant, differentiating equation (1), combining it with equation (2), and normalizing the result to obtain an equation describing damped, forced oscillations of the scaled extrusion velocity, $u' = u/[(Q - RB)/A]$:

$$(1 + Kt') \frac{d^2 u'}{dt'^2} + 2D \frac{du'}{dt'} + \frac{u'}{V'} = \frac{1}{V'} - \frac{Kgt_0}{(Q - RB)/A} \quad (4)$$

Here $t' = t/t_0$, $V' = V/V_0$, and quantities that largely control plug motion are the characteristic time, t_0 , dimensionless mass change rate, K , and dimensionless damping, D :

$$t_0 = \frac{[m_0(\alpha_1 + \alpha_2)V_0]^{1/2}}{A}, \quad K = \frac{\kappa t_0}{m_0}, \quad (5)$$

$$D = K + \frac{1}{2} \frac{t_0}{m_0} \frac{dF}{du}$$

In the simple case in which $K = 0$, $V = V_0$, and D is constant (implying that F is a linear function of u), solutions of equation (4) indicate that u' either equals 1 (the steady equilibrium state) or oscillates about equilibrium with period $T = 2\pi t_0$. This formula yields reasonable predictions of the period between drumbeat earthquakes at MSH (Supplementary Fig. 2), but a model as simple as equation (4) with constant D cannot explain drumbeat persistence because it predicts that oscillations in extrusion rate grow unstably if $D < 0$, decay to a stable, steady state if $D > 0$, and remain unchanged only in the improbable case with $D = 0$. These inferences are modified only slightly if $K \neq 0$ or $V \neq V_0$.

Persistent oscillations are much more probable if D varies as a consequence of nonlinearly rate-dependent friction, which produces variable feedback. To illustrate effects of such feedback we use a simple nonlinear friction rule:

$$F = \text{sgn}(u) F_0 (1 - c \sinh^{-1} |u/u_{\text{ref}}|) \quad (6)$$

in which $\text{sgn}(u)$ denotes the sign of u , F_0 is the friction force at static limiting equilibrium (for details, see Supplementary Information), c is a rate-weakening parameter ($c \ll 1$), and u_{ref} is a reference value of u (Supplementary Fig. 3). This function mimics key aspects of MSH fault-gouge friction measured in experiments¹³, but it omits evolving state variables included in more elaborate friction models²⁶. Equation (6) does, however, include a fundamental type of state dependence: if oscillations lead to $u = 0$, F abruptly changes from positive to negative because gravity provides a potential for downward plug motion, which friction opposes. When F jumps, damping becomes infinite and prohibits downward settling of the plug, thereby transforming oscillatory instability to stick-slip instability (Supplementary Fig. 4).

Numerical solutions of equations (1)–(3) using a Runge-Kutta method²⁷ and incorporating equation (6) show how stick-slip cycles are regulated during extrusion. In the examples discussed here (with $K = 0$, $B = Q = 2 \text{ m}^3 \text{ s}^{-1}$, $T = 10 \text{ s}$ and $u_{\text{ref}} = 0.1(Q/A)$), values of D at the equilibrium slip rate $u_0 = Q/A$ completely determine the behaviour of solutions. As the magnitude of D increases, slip events become less frequent and more abrupt, and simultaneous evolution of u and p reveals key features of the system's dynamics (Fig. 5). When basal magma influx produces pressure exceeding the static equilibrium value, it triggers slip at a rate that depends on D . When the

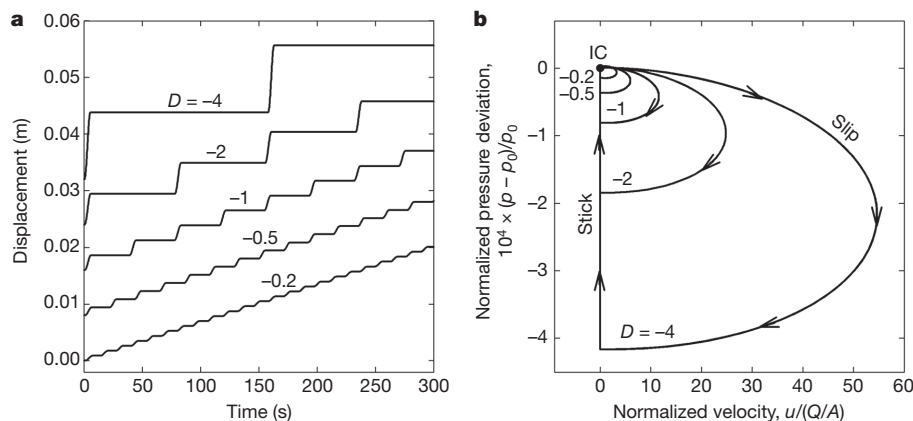


Figure 5 | Calculated stick-slip extrusion behaviour. Computations employed D values obtained by using equation (6) to find $[dF/du]_{u=u_0} = -F_0 c / u_{\text{ref}} [1 + (u_0/u_{\text{ref}})^2]^{-1/2}$ and substituting this result in equation (5). Results are depicted as time series (a), and as limit cycles in the velocity–pressure phase plane (b). Arrows in b point in the direction of

advancing time. Initial conditions (IC) for these calculations represent static limiting equilibrium specified by $u = 0$, $p = p_0 = (m_0 g + F_0)/A = 1.2936 \times 10^7 \text{ Pa}$, $V = V_0 = 6.32 \times 10^5 \text{ m}^3$ and $\rho = \rho_0 = 2,000 \text{ kg m}^{-3}$.

effects of diminishing magma pressure and plug inertia no longer exceed the effects of gravity and friction, slip terminates and stick begins. Magma pressure then rebuilds until it triggers additional slip.

Computations with $D = -2$ produce stick-slip cycles with amplitudes and periods similar to those inferred for MSH plug extrusion (Fig. 5 and Supplementary Fig. 5). With $D = -2$, individual slip events entail about 5 mm of displacement in about 5 s, maximum slip rates of $\sim 2 \text{ mm s}^{-1}$, and about 10^8 J of work done against friction. Attendant fluctuations in magma pressure are $< 0.02\%$ of p_0 , equivalent to only $\sim 2,400 \text{ Pa}$ or $< 0.2 \text{ m}$ of static magma pressure head. This result is insensitive to variations in the parameters constituting D , provided that t_0 is unchanged (Supplementary Figs 6 and 7), and multiplied by $A = 30,000 \text{ m}^2$, the pressure change also serves as a proxy for the force drop responsible for generating seismicity ($\sim 7 \times 10^7 \text{ N}$). A large fraction of this force drop occurs almost instantaneously, facilitating radiation of seismic energy (Supplementary Fig. 5).

Discussion

All silicic volcanic eruptions that follow a period of repose begin with a plugged conduit. Commonly the conduit is rapidly cleared of solid rock, and a profoundly disequibrated state exists as magma reaches the surface. In the 2004–05 eruption of MSH, the conduit remained plugged by solid rock that was pushed upward by ascending, solidifying magma. The magma–plug system reached a sustained, near-equilibrium state characterized by nearly steady extrusion of gouge-coated dacite and nearly periodic shallow earthquakes. A dynamical model of the magma–plug system produces output consistent with the hypothesis that these drumbeat earthquakes resulted from repetitive stick-slip motion along the margins of the extruding plug, and that the stick-slip cycles represent mechanical oscillations about equilibrium. Application of driving force by an unusually compliant crustal body (that is, bubbly magma) enables stick-slip events to be large enough to produce earthquakes at the shallow focal depths ($< 1 \text{ km}$) observed at MSH. If gouge displacement were driven by a stiffer body (that is, solid rock), oscillations in extrusion rate would be smaller, more frequent, and more likely to be aseismic.

Evidence that the 2004–05 eruption of MSH quickly settled into a persistent, near-equilibrium, oscillatory state implies that magma pressure never deviated much from the equilibrium pressure (Supplementary Fig. 8). Moreover, absence of deep earthquakes and minimal far-field deformation imply minimal changes in the magmatic system at depth, and we infer that the volcano was probably poised in a near-eruptive equilibrium state long before the onset of the 2004–05 eruption. In many respects, the 2004–05 eruption can be viewed as a continuation of the dome-building eruption of 1980–86, whereas the explosive eruption of 18 May 1980 differed greatly because it was triggered by a 2.5 km^3 landslide that rapidly depressurized volatile-rich magma.

Received 7 April; accepted 3 October 2006.

- Sparks, R. S. J. The causes and consequences of eruptions of andesite volcanoes: opening remarks. *Phil. Trans. R. Soc. Lond. A* **358**, 1435–1440 (2000).
- Lahr, J. C., Chouet, B. A., Stephens, C. D., Power, J. A. & Page, R. A. Earthquake classification, location, and error analysis in a volcanic environment: implications for the magmatic system of the 1989–1990 eruptions at Redoubt Volcano, Alaska. *J. Volcanol. Geotherm. Res.* **62**, 137–151 (1994).
- Neuberg, J. Characteristics and causes of shallow seismicity in andesite volcanoes. *Phil. Trans. R. Soc. Lond. A* **358**, 1533–1546 (2000).
- Mullineaux, D. R. & Crandell, D. R. in *The 1980 Eruptions of Mount St. Helens, Washington* (eds Lipman, P. L. & Mullineaux, D. R.) 3–15 (USGS Professional Paper 1250, US Geological Survey, Washington DC, 1981).
- Swanson, D. A. & Holcomb, R. T. in *Lava Flows and Domes* (ed. Fink, J.) 3–24 (Springer, Berlin, 1990).
- Mastin, L. G. Explosive tephra emissions at Mount St. Helens, 1989–1991; the violent escape of magmatic gas following storms? *Geol. Soc. Am. Bull.* **106**, 175–185 (1994).
- Moran, S. C. Seismicity at Mount St. Helens, 1987–1992: Evidence for repressurization of an active magmatic system. *J. Geophys. Res.* **99**, 4341–4354 (1994).
- Dzurisin, D., Vallance, J. W., Gerlach, T. M., Moran, S. C. & Malone, S. D. Mount St. Helens reawakens. *Eos* **86**, 25; 29 (2005).
- Schilling, S. P., Carrara, P. E., Thompson, R. A. & Iwatsubo, E. Y. Posteruption glacier development within the crater of Mount St. Helens, Washington, USA. *Quat. Res.* **61**, 325–329 (2004).
- Walder, J. S., LaHusen, R. G., Vallance, J. W. & Schilling, S. P. Crater glaciers on active volcanoes: hydrological anomalies. *Eos* **86**, 521; 528 (2005).
- Pallister, J. S., Reagan, M. & Cashman, K. A new eruptive cycle at Mount St. Helens? *Eos* **86**, 499 (2005).
- Tuffen, H. & Dingwell, D. Fault textures in volcanic conduits: evidence for seismic trigger mechanisms during silicic eruptions. *Bull. Volcanol.* **67**, 370–387 (2005).
- Moore, P. L., Iverson, N. R. & Iverson, R. M. Frictional properties of the Mount St. Helens gouge. In *A Volcano Rekindled: The First Year of Renewed Eruption at Mount St. Helens, 2004–2005* (eds Sherrod, D. A. & Scott, W. E.) (USGS Professional Paper, US Geological Survey, submitted).
- Blundy, J. & Cashman, K. Ascent-driven crystallization of dacite magmas at Mount St. Helens, 1980–1986. *Contrib. Mineral. Petrol.* **140**, 631–650 (2001).
- McGee, K. A., Doukas, M. P. & Gerlach, T. M. Quiescent hydrogen sulfide and carbon dioxide degassing from Mount Baker, Washington. *Geophys. Res. Lett.* **28**, 4479–4482 (2001).
- Newman, S. & Lowenstern, J. A. VolatileCalc: a silicate melt–H₂O–CO₂ solution model written in Visual Basic for Application (VBA) with Microsoft® Excel. *Comput. Geosci.* **28**, 597–604 (2002).
- Rutherford, M. J. Experimental petrology applied to volcanic processes. *Eos* **74**, 49; 55 (1993).
- Yang, X., Davis, P. M. & Dieterich, J. H. Deformation from inflation of a dipping finite prolate spheroid in an elastic half space as a model for volcanic stressing. *J. Geophys. Res.* **93**, 4249–4257 (1988).
- Melnik, O. E. & Sparks, R. S. J. Nonlinear dynamics of lava dome extrusion. *Nature* **402**, 37–41 (1999).
- Mason, R. M., Starostin, A. B., Melnik, O. E. & Sparks, R. S. J. From Vulcanian explosions to sustained explosive eruptions: the role of diffusive mass transfer in conduit flow dynamics. *J. Volcanol. Geotherm. Res.* **153**, 148–165 (2006).
- Chouet, B. Long-period volcano seismicity: its source and use in eruption forecasting. *Nature* **380**, 309–316 (1996).
- Denlinger, R. P. & Hoblitt, R. P. Cyclic eruptive behavior of silicic volcanoes. *Geology* **27**, 459–462 (1999).
- Voight, B. et al. Magma flow instability and cyclic activity at Soufriere Hills Volcano, Montserrat, British West Indies. *Science* **283**, 1138–1142 (1999).
- Ozerov, A., Ispolatov, I. & Lees, J. Modeling Strombolian eruptions of Karymsky volcano, Kamchatka, Russia. *J. Volcanol. Geotherm. Res.* **122**, 265–280 (2003).
- Mastin, L. G. & Ghiorso, M. S. *A Numerical Program for Steady-state Flow of Magma-gas Mixtures through Vertical Eruptive Conduits* (USGS Open-File Report 00–209, US Geological Survey, Vancouver, Washington, 2000).
- Marone, C. Laboratory-derived friction laws and their application to seismic faulting. *Annu. Rev. Earth Planet. Sci.* **26**, 643–696 (1998).
- Press, W. H., Flannery, B. P., Teukolsky, S. A. & Vetterling, W. T. *Numerical Recipes* (Cambridge Univ. Press, Cambridge, UK, 1986).

Supplementary Information is linked to the online version of the paper at www.nature.com/nature.

Acknowledgements We are indebted to many colleagues in the USGS Volcano Hazards Program and the Pacific Northwest Seismic Network who contributed to hazard assessment and study of the ongoing eruption at MSH.

Author Information Reprints and permissions information is available at www.nature.com/reprints. The authors declare no competing financial interests. Correspondence and requests for materials should be addressed to R.M.I. (riverson@usgs.gov), D.Z. (dzurisin@usgs.gov) or C.A.G. (cgardner@usgs.gov).